Lumbar Fusion including Sacroiliac Joint Fixation Increases the Stress and Angular Motion at the Hip Joint: A Finite Element Study

Takuhei Kozaki[1], Hiroshi Hashizume[1], Hiroyuki Oka[2], Satoru Ohashi[3], Yoh Kumano[4], Ei Yamamoto[5], Akihito Minamide[1], Yasutsugu Yukawa[1], Hiroshi Iwasaki[1], Shunji Tsutsui[1], Masanari Takami[1], Keiji Nakata[1], Takaya Taniguchi[1], Daisuke Fukui[1], Daisuke Nishiyama[1], Manabu Yamanaka[1], Hidenobu Tamai[1], Ryo Taiji[1], Shizumasa Murata[1], Akimasa Murata[1] and Hiroshi Yamada[1]

1) Department of Orthopaedic Surgery, Wakayama Medical University, Wakayama, Wakayama, Japan
2) Department of Medical Research and Management for Musculoskeletal Pain, Faculty of Medicine, 22nd Century Medical and Research Center, The University of Tokyo, Tokyo, Japan
3) Department of Orthopaedic Surgery, Sagamihara Hospital, National Hospital Organization, Sagamihara, Kanagawa, Japan
4) Department of Spine Surgery, Tokyo Yamate Medical Center, Japan Community Healthcare Organization, Tokyo, Japan
5) Department of Biomedical Engineering, Faculty of Biology-Oriented Science and Technology, KinDai University, Kinokawa, Wakayama, Japan

Abstract:

Introduction: Adult spinal fusion surgery improves lumbar alignment and patient satisfaction. Adult spinal deformity surgery improves saggital balance not only lumbar lesion, but also at hip joint coverage. It was expected that hip joint coverage rate was improved and joint stress decreased. However, it was reported that adjacent joint disease at hip joint was induced by adult spinal fusion surgery including sacroiliac joint fixation on an X-ray study. The mechanism is still unclear. We aimed to investigate the association between lumbosacral fusion including sacroiliac joint fixation and contact stress of the hip joint.

Methods: A 40-year-old woman with intact lumbar vertebrae underwent computed tomography. A three-dimensional non-linear finite element model was constructed from the L4 vertebra to the femoral bone with triangular shell elements (thickness, 2 mm; size, 3 mm) for the cortical bone's outer surface and 2-mm (lumbar spine) or 3-mm (femoral bone) tetrahedral solid elements for the remaining bone. We constructed the following four models: a non-fusion model (NF), a L4-5 fusion model (L5F), a L4-S1 fusion model (S1F), and a L4-S2 alar iliac screw fixation model (S2F). A compressive load of 400 N was applied vertically to the L4 vertebra and a 10-Nm bending moment was additionally applied to the L4 vertebra to stimulate flexion, extension, left lateral bending, and axial rotation. Each model's hip joint's von Mises stress and angular motion were analyzed.

Results: The hip joint's angular motion in NF, L5F, S1F, and S2F gradually increased; the S2F model presented the greatest angular motion.

Conclusions: The average and maximum contact stress of the hip joint was the highest in the S2F model. Thus, lumbosacral fusion surgery with sacroiliac joint fixation placed added stress on the hip joint. We propose that this was a consequence of adjacent joint spinopelvic fixation. Lumbar-to-pelvic fixation increases the angular motion and stress at the hip joint.

Introduction

The prevalence of adult spinal deformity surgery has recently increased, in line with the increasingly aging population[1]. Adult spinal fusion surgery improves lumbar alignment and hip joint coverage rate[2], which is expected to decrease the stress on the hip joint[3,4]. However, a recent clinical study reported that hip joint pain increased after adult spinal deformity surgery[5]. Currently, sacroiliac screws are used to prevent distal junctional failure in adult spinal deformity surgery[6,7]. A radiographic study showed that sacroiliac joint fixation using a sacroiliac joint screw impacted the hip joint after adult spinal deformity surgery in 118 patients based on an X-ray study[8]. Adjacent segment disease (ASD) has also been reported as one of the major complications of spinal fusion surgery. The proposed mechanism for ASD is that mobility is transferred from the fused segment to the next mobile segment. Lumbosacral joint disease and sacroiliac joint pathology have been observed after lumbar fusion and lumbosacral fusion surgeries, respectively[9]. Similarly, it has been suspected that the load on the hip joint is increased after spinal fusion surgery, including the sacroiliac joint, which reduces the mobility of the lumbar spine and pelvis. Therefore, in this study we compared the contact pressure of the hip joint with or without sacroiliac joint fixation.

Materials and Methods

This study was approved by the ethics committee of
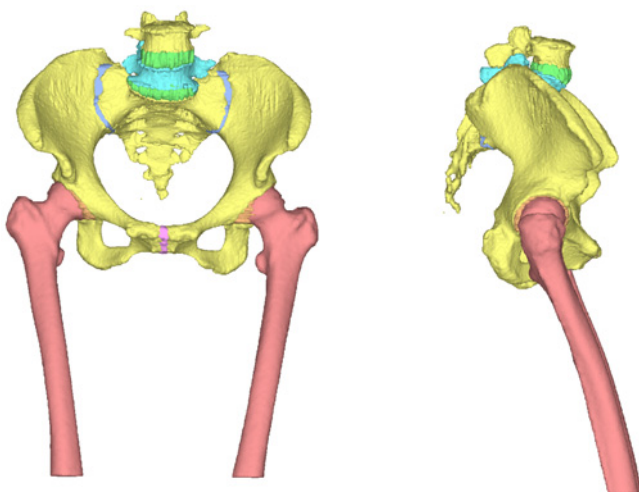
Figure 1. Finite element model from the L4 vertebra to the femoral bone.

Wakayama Medical University. The participant provided written informed consent. A 40-year-old woman with a benign soft tissue tumor at her ankle underwent computed tomography (CT) from the lumbar spine to the lower limb with simultaneous scanning of a calibration phantom (BMAS 200; Kyoto Kagaku, Kyoto, Japan) containing hydroxyapatite rods to determine bone density.

A three-dimensional nonlinear finite element (FE) model was constructed from the patient's DICOM data and analyzed with the Mechanical Finder® version 10.0 software (RCCM, Tokyo, Japan). FE models, which were constructed from the L4 vertebra to the femoral bone, were equipped with triangular shell elements (thickness, 2 mm; size, 3 mm) for the outer surface of the cortical bone and tetrahedral solid elements with a size of 1.5 mm for the hip joint cartilage and 2 mm for the rest of the elements (Fig. 1). The Young's modulus for the pelvis, femur, and lumbar spine was determined using the equations proposed in a previous study[10] and the Poisson's ratios were 0.40. These equations are used as follows to calculate Young's modulus (E) from bone density (ρ):

$E=0.01$ (ρ=0)
$E=33900\rho^{2.20}$ (0<ρ≤0.27)
$E=5307\rho+469$ (0.27<ρ<0.6)
$E=10200\rho^{2.01}$ (0.6≤ρ)

To calculate bone density from CT values, the following set of equations was used:

ρ (g/cm³)=(CT number+1.4246)×0.001/1.058
(If the CT number>−1 Hounsfield unit [HU])
ρ (g/cm³)=0
(If the CT number ≤;−1 HU)

FE model - validation

Lumbar spine functionally was validated against previous research[11]. The experimental study simulated motions as follows: flexion, extension, axial rotation, and lateral bending. The same boundary conditions and moment were applied to the current model as follows: the sacrum was constrained and an L4-sacrum intact model was used. The ROMs of the flexion, extension, axial rotation, and lateral bending were favorably compared with the previous experimental study (Fig. 2a). Next, the sacroiliac joint was validated against a previous cadaveric experimental study[12]. We compared the ROM of the FE intact model with the previous study at stance and swing phase. The predicted data were well fitted with the past study. Therefore, we concluded that our FE model would provide reasonable comparative parameters (Fig. 2b). Finally, we compared hip stress on FE intact

(a)   (b)
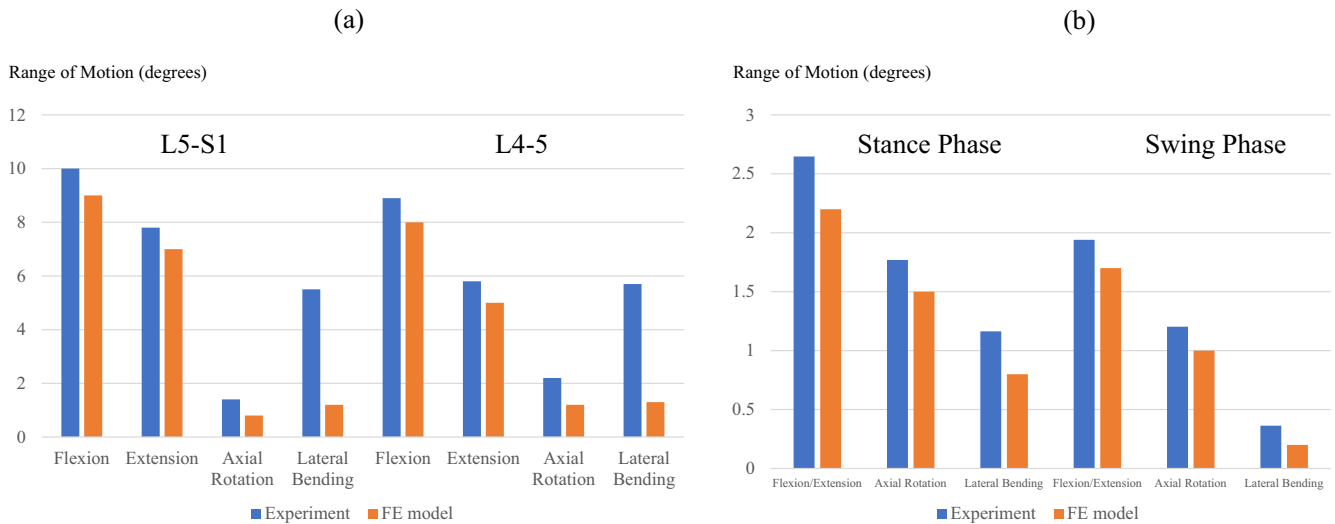
Figure 2. (a) The range of motion of the lumbar and sacrum of our model were validated with a previous cadaveric study [11]. (b) The range of motion of the sacroiliac joint of our model was validated with a previous cadaveric study [12].

Table 1. The von Mises stress on the Hip Joint Was Compared with Past Hip Finite Element Model [13].

Peak contact stress (MPa)			
Past study		FE model	
CE angle 26 (between 8 and 41)	CE angle −4 (between −36 and 14)	CE angle 25	CE angle 0
2.8 (1.8 to 3.6)	4.1 (2.7 to 6.6)	2.4	3.5

model with a previous FE model[13]. It was reported that the hip stress decreased as the center edge (CE) angle of the hip increased when 1800 N was applied. We created two models, one was intact hip model (CE angle 25) and the other was lower coverage model (CE angle 0). The predicted von Mises stress was similar to that in the previous study[13] (Table 1).

Model

We constructed four models, which were different from the lower instrumented vertebrae, as follows: a non-fusion model (NF) (Fig. 1), an L4-5 fusion model (L5F), an L4-S1 fusion model (S1F), and an L4-S2 alar iliac screw fixation model (S2F). Segments were fused using titanium cages and graft bone with posterior fusion. Each screw was connected to the titanium rod, which was modeled using Metasequoia® version4 (Tetraface, Tokyo, Japan). A compressive load of 400 N was applied vertically to the L4 vertebra and an additional 10 Nm bending moment was applied to the L4 vertebra to stimulate the flexion, extension, left lateral bending, and axial rotation. The distal femoral bone side was completely restrained. The entire hip joint cartilage was placed on the side of the acetabular roof. The material properties are listed in Table 2[14-16]. Young's moduli and Poisson's ratios for the lumbar vertebra, pelvis, and femoral bone were determined using the equations previously proposed[17]. The hip

joint was used for contact analysis.

FE analysis was performed to measure the average and maximum stress in the acetabular cartilage of the hip joint. The von Mises stress and angular motion of the hip joint were analyzed in each model. We defined maximum stress as the greatest stress at whole of the hip cartilage and mean stress as the average of the whole hip joint cartilage. The angular motion was calculated as follows: the anterior pelvic plane angle was used for flexion, extension, and rotation. The angle between the line of both the anterior superior iliac spine and the horizontal line was measured for left lateral bending.

Results

The stress at the hip joint cartilage and angular motion were gradually increased as fusion segments increased in all postures (Fig. 3, 4, 5).

Stress and angular motion at flexion

The von Mises stress at the hip joint was greatest in the S2F model (Fig. 6). The mean of the average von Mises stress at both sides of the hip joint in flexion increased by 51.5% ($1.0×10^{-1}$ MPa) in the S2F model, 7.5% ($0.71×10^{-1}$ MPa) in the S1F model, and 6.1% ($0.70×10^{-1}$ MPa) in the L5F model compared with the NF model ($0.66×10^{-1}$ MPa).

Table 2. Material Properties.

Material	Stiffness coefficient (N/m)
Anterior longitudinal ligament	0 (ε<0), 49.7 (ε<12), 127.4 (12<ε)
Posterior longitudinal ligament	0 (ε<0), 20.0 (ε<11), 40.0 (11<ε)
Ligamentum flavum	0 (ε<0), 60.0 (ε<6.2), 78.0 (6.2<ε)
Transverse ligament	0 (ε<0), 1.8 (ε<18), 10.6 (18<ε)
Capsular ligament	0 (ε<0), 22.5 (ε<25), 98.7 (25<ε)
Interspinous ligament	0 (ε<0), 40.0 (ε<14), 46.4 (14<ε)
Supraspinous ligament	0 (ε<0), 19.2 (ε<20), 48.0 (20<ε)
Sacrospinous ligament	1400
Sacrotuberous ligament	1500
Interosseous ligament	2800
Sacroiliac anterior ligament	700
Sacroiliac posterior ligament (long)	1000
Sacroiliac posterior ligament (short)	400
Iliolumbar ligament	1000
Pubicum superius ligament	500
Pubis arcuate ligament	500
Gluteus maximus	344
Gluteus medius	779
Gluteus minimus	660
Psoas	100
Adductor magnus	257
Adductor longus	134
Adductor brevis	499

Material	Elastic modulus (MPa)	Poisson's ration
Fibrous rings	450	0.45
Vertebral pulp	2.25	0.4995
Sacrum cartilage	54	0.4
Pubic symphysis	5	0.45
Acetabulum cartilage	12	0.42
Bone graft	3500	0.25
Implant (Titanium)	110000	0.3

The mean of the maximum von Mises stress at both sides of the hip joint in flexion increased by 69.3% (2.15 MPa) in the S2F model, 10.2% (1.40 MPa) in the S1F model, and 7.8% (1.37 MPa) in the L5F model compared with the NF model (1.27 MPa). The angular motion also increased with the increase in the number of levels fused. The angular motion at the hip joint increased by 1.16° in the S2F model (1.5°), 0.44° in the S1F model (0.78°), and 0.05° in the L5F model (0.39°) compared with the NF model (0.34°).
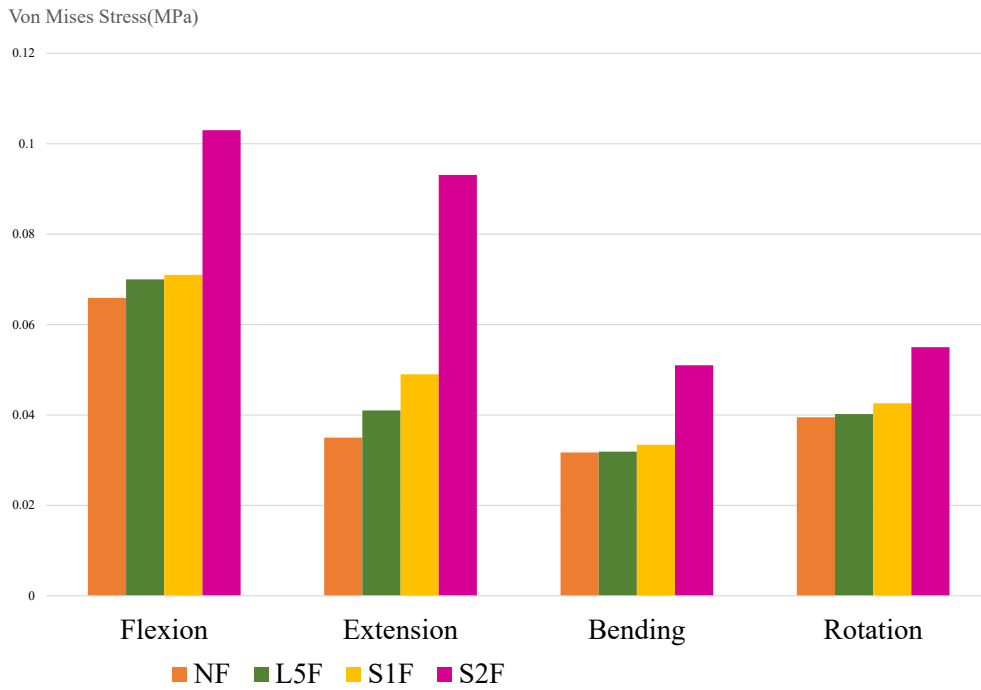
Stress and angular motion at extension

The von Mises stress and angular motion at the hip joint in extension was similar to that in flexion. The mean of the average von Mises stress at both sides of the hip joint in extension increased by 2.7 times (0.93×10⁻¹ MPa) in the S2F model, 40.0% (0.49×10⁻¹ MPa) in the S1F model, and 17.1% (0.41×10⁻¹ MPa) in the L5F model, compared with the NF model (0.35×10⁻¹ MPa). The mean of the maximum von Mises stress at both sides of the hip joint in extension increased by 3.6 times (1.93 MPa) in the S2F model, 72.2% (0.93 MPa) in the S1F model, and 3.7% (0.56 MPa) in the

L5F model, compared with the NF model (0.54 MPa). Angular motion at the hip joint in extension increased by 1.91° in the S2F model (2.36°), 0.72° in the S1F model (1.17°), and 0.05° in the L5F model (0.50°), compared with the NF model (0.45°).

Stress and angular motion at bending

The stress at the hip joint cartilage and angular motion was gradually increased as the bending of fusion segments increased, but the difference among models was smaller than those in flexion and extension. The mean of the average von Mises stress at both sides of the hip joint in bending increased by 64.5% (0.51×10⁻¹ MPa) in the S2F model, 6.5% (0.33×10⁻¹ MPa) in the S1F model, and 3.2% (0.32×10⁻¹ MPa) in the L5F model, compared with the NF model (0.31 ×10⁻¹ MPa). The mean of the maximum von Mises stress at both sides of the hip joint in bending increased by twice (1.0 MPa) in the S2F model, 20.0% (0.60 MPa) in the S1F model, and 12.0% (0.56 MPa) in the L5F model, compared with the NF model (0.50 MPa). The angular motion at the hip joint increased by 0.72° in the S2F model (0.84°), 0.17°

Figure 3. Mean of the average von Mises stress at both sides of the hip joint cartilage.
NF: non-fusion model, L5F: L4-5 fusion model, S1F: L4-S1 fusion model, S2F: L4-S2 alar screw fixation model
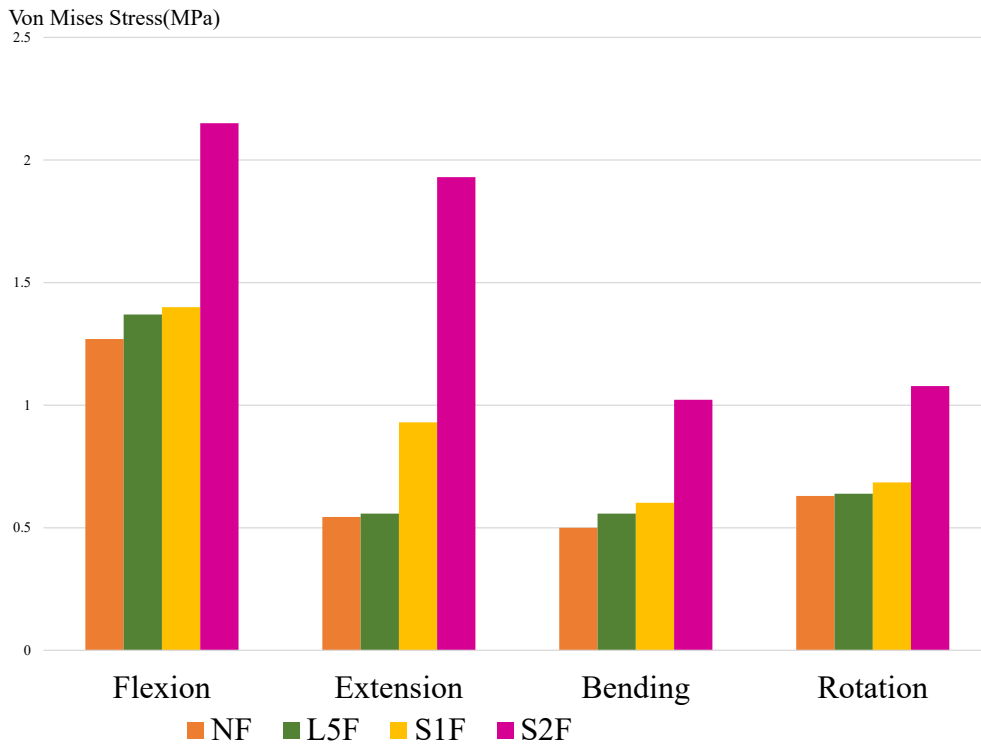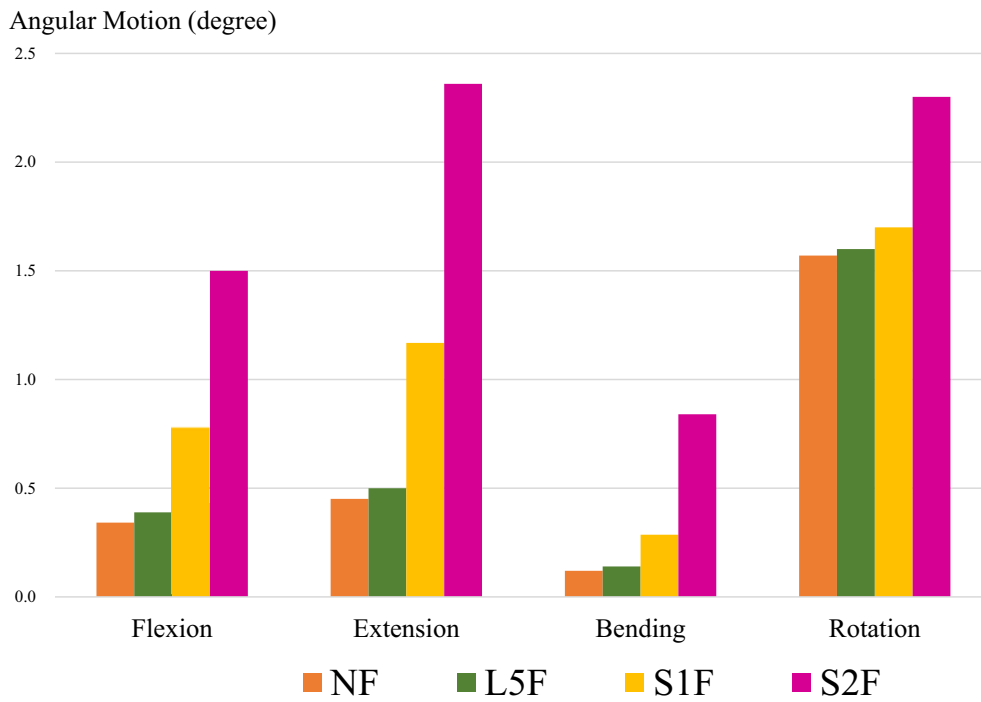

Figure 4. Mean of the peak von Mises stress at both sides of the hip joint cartilage.
NF: non-fusion model, L5F: L4-5 fusion model, S1F: L4-S1 fusion model, S2F: L4-S2 alar screw fixation model

in the S1F model (0.29°), and 0.01° in the L5F model (0.13°), compared with the NF model (0.12°).

Stress and angular motion during rotation

The tendencies during rotation were similar to the other

Angular Motion (degree)

Figure 5. Mean of the average angular motion at both sides of the hip joint cartilage.
NF: non-fusion model, L5F: L4-5 fusion model, S1F: L4-S1 fusion model, S2F: L4-S2 alar screw fixation model
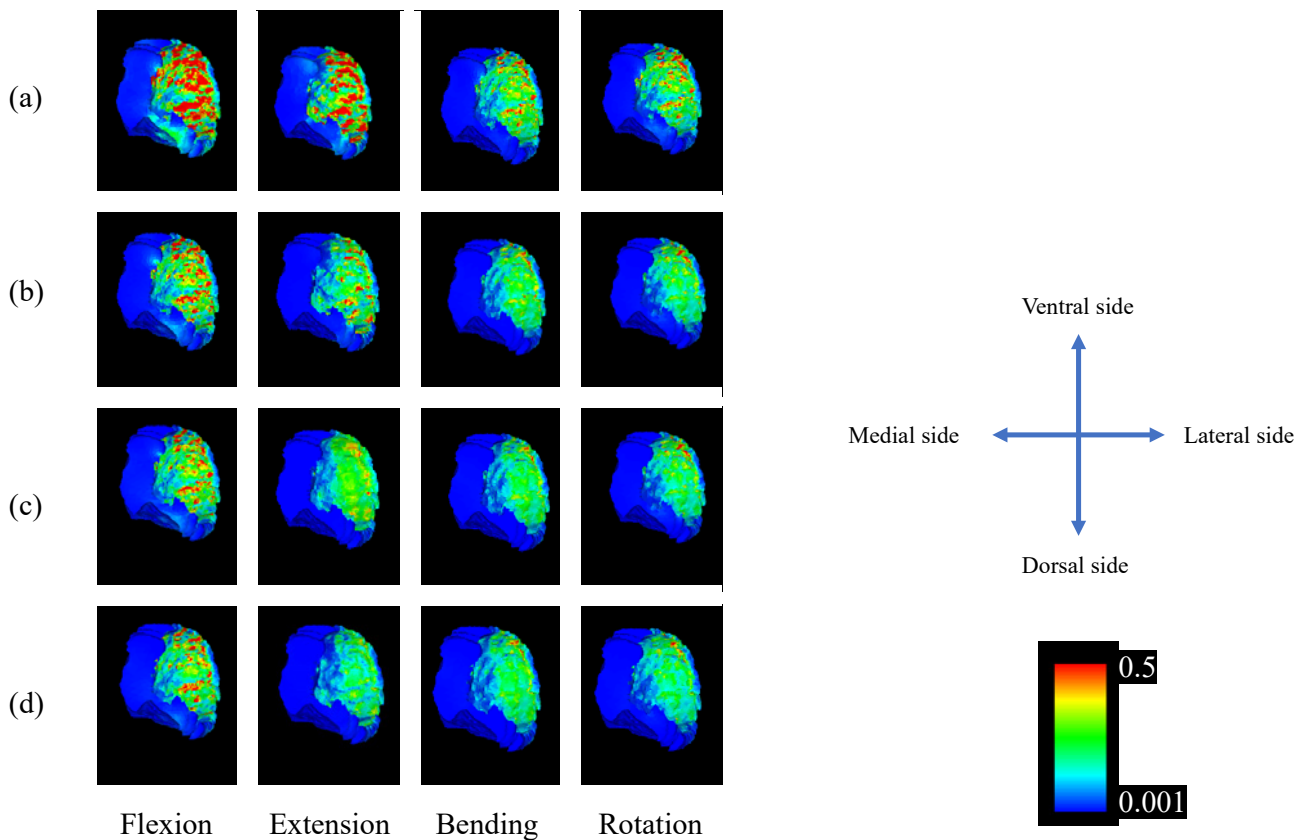
Figure 6. Stress contours at the left hip cartilage in the L4-S2 fixation model (a), L4-S1 fixation model (b), L4-L5 fixation model (c), and non-fixation model (d) at flexion, extension, bending, and rotation.

motions, but smaller differences in von Mises stress and angular motion were observed compared with flexion and extension. The mean of the average von Mises stress at both sides of the hip joint in rotation increased by 41.0% (0.55×

10^{-1} MPa) in the S2F model, 7.7% (0.42×10^{-1} MPa) in the S1F model, and 2.6% (0.40×10^{-1} MPa) in the L5F model, compared with the NF model (0.39×10^{-1} MPa). The mean of the maximum von Mises stress at both sides of the hip joint in rotation increased by 74.6% (1.1 MPa) in the S2F model, 9.5% (0.69 MPa) in the S1F model, and 1.6% (0.64 MPa) in the L5F model, compared with the NF model (0.63 MPa). The angular motion at the hip joint increased by 0.73° in the S2F model (2.3°), 0.13° in the S1F model (1.7°), and 0.03° in the L5F model (1.6°), compared with the NF model (1.57°).

Discussion

This study revealed the influence of lower instrumented vertebrae on the acetabular cartilage of the hip joint, especially during L4-S2 alar iliac screw fixation, which had the greatest impacted on the hip joint. A previous study reported that spinal fusion surgery added stress to the adjacent spinal segment and sacroiliac joint[9,18]. Adult spinal deformity surgery, including sacroiliac joint fixation, has also been shown to influence the hip joint in a radiographical study[8]. Our results support these previous findings and suggest that adult spinal fusion surgery, including S2 alar iliac screw fixation, may contribute to osteoarthritis of the hip joint.

One of the major complications of adult spinal fusion surgery is ASD. ASD typically develops at the mobile segment above or below the fused spine[19]. Lumbar fusion surgery has been reported to increase mobility in the proximal and distal adjacent segments and add stress on the facet and disc in adjacent mobile segments[20]. This was thought to be caused by the transfer of motion from the fused segments to the next mobile intact segments[21]. Using single-photon emission computed tomography and bone scintigraphy, lumbosacral fusion was shown to induce sacroiliac joint dysfunction[22]. In this study we observed increased uptake in the sacroiliac joint, reflecting mechanical overloading and sacroiliitis. Similarly, hip joint pain after spinal fusion surgery has been reported[5]. A radiological study reported that sacroiliac joint fixation in adult spinal fusion surgery decreased the amount of cartilage in the hip joint[8]. In our FE study, it was clear that lumbosacral fusion led to a greater increase in the angular motion and stress on the sacroiliac joint than lumbar fusion, which does not include pelvic fixation. This study also revealed that the contact pressure of the hip joint was the highest in the S2F model. The hip joint lesion after lumbar fusion, including sacroiliac joint fixation, was thought to be a type of ASD.

Several studies have revealed increases in the angular motion of adjacent segments in ASD. Similar to ASD, the sacroiliac joint had increased angular motion in the lumbosacral fusion model than in the lumbar fusion models[23]. In this study, the angular motion of the pelvis was greater in the S2F model than in the other lumbar or lumbosacral fusion models. In clinical reports, a hip-spine relation has been reported[24]. Patients with stiff spines caused by degenerative disc disease experience less spinal mobility and more hip motion during sit-to-stand and stand-to-sit motions. Reduced hip motion can be compensated for by spinal mobility, and decreased mobility of the thoracolumbar level is associated with the progression of hip osteoarthritis[25]. Therefore, decreased spinal mobility can be a risk factor for hip osteoarthritis progression by potentially increasing the mechanical load on the hip[26]. In this study, lumbosacral fusion, including sacroiliac joint fixation, induced less lumbar mobility and greater hip motion, which induced greater angulation and greater stress on the hip joint.

This study has several limitations. First, the contact between the screw surfaces and bone was simulated as a complete fusion, but it did not reflect this fact. Hip joint degeneration could have been influenced by various factors, such as gender, body mass index, and coverage rate. Moreover, the hip joint has a broad variation in formation and degenerative change, but we used the ideal model to assess the impact of lumbar fusion and sacroiliac fixation on the hip joint. Adult spinal deformity surgery often fuses the vertebra from the lower thoracic spine to the pelvis, but our model was constructed from the L4 vertebra. This was because the model from the lower thoracic to the femur was too large and could not be analyzed. The von Mises stress and angular motion at the hip joint were highest in the S2F model, but there was little difference in bending and rotation. However, this trend is in agreement with previous findings[23]. We have taken various postures in daily activities by combining flexion, extension, bending, and rotation postures, However, these motions did not reflect the daily motion, for example standing, sitting, or walking. So, research based on motion analysis is necessary. This study was based on a single standardized model, which might not be fitted to various patients. However, this FE model was validated against previous research and the result was favorable.

In conclusion, lumbar fusion with sacroiliac joint screw fixation leads to more angular motion and contact stress on the hip joint than the other models without sacroiliac joint fixation. Therefore, clinicians should be concerned with hip lesions after lumbo-pelvic fixation surgery.

References

1. Swank S, Lonstein JE, Moe JH, et al. Surgical treatment of adult scoliosis. A review of two hundred and twenty-two cases. J Bone Joint Surg Am. 1981;63(2):268-87.
2. Fukushima K, Miyagi M, Inoue G, et al. Relationship between spinal sagittal alignment and acetabular coverage: a patient-matched control study. Arch Orthop Trauma Surg. 2018;138(11): 1495-9.
3. Knight SJ, Abraham CL, Peters CL, et al. Changes in chondrolabral mechanics, coverage, and congruency following peri-acetabular osteotomy for treatment of acetabular retroversion: a patient-specific finite element study. J Orthop Res. 2017;35(11): 2567-76.
4. Kitamura K, Fujii M, Utsunomiya T, et al. Effect of sagittal pelvic tilt on joint stress distribution in hip dysplasia: a finite element analysis. Clin Biomech. (Bristol, Avon). 2020;74:34-41.
5. Si G, Li T, Liu X, et al. Correlation analysis between postoperative hip pain and spino-pelvic/hip parameters in adult scoliosis patients after long-segment spinal fusion. Eur Spine J. 2020;29(12): 2990-7.
6. Hasan MY, Liu G, Wong HK, et al. Postoperative complications of S2AI versus iliac screw in spinopelvic fixation: a meta-analysis and recent trends review. Spine J. 2020;20(6):964-72.
7. Hyun SJ, Jung JM, Kim KJ, et al. Durability and failure types of S2-alar-iliac screws: an analysis of 312 consecutive screws. Oper Neurosurg (Hagerstown). 2020;20(1):91-7.
8. Kozaki T, Hashizume H, Nishiyama D, et al. Adjacent segment disease on hip joint as a complication of spinal fusion surgery including sacroiliac joint fixation. Eur Spine J. 2021;30(5):1314-9.
9. Park P, Garton HJ, Gala VC, et al. Adjacent segment disease after lumbar or lumbosacral fusion: review of the literature. Spine (Phila Pa 1976). 2004;29(7):1938-44.
10. Keyak JH, Rossi SA, Jones KA, et al. Prediction of femoral fracture load using automated finite element modeling. J Biomech. 1998;31(2):125-33.
11. Yamamoto I, Panjabi MM, Crisco T, et al. Three-dimensional movements of the whole lumbar spine and lumbosacral joint. Spine (Phila Pa 1976). 1989;14(11):1256-60.
12. Lindsey DP, Parrish R, Gundanna M, et al. Biomechanics of unilateral and bilateral sacroiliac joint stabilization: laboratory investigation. J Neurosurg Spine. 2018;28(3):326-32.
13. Ike H, Inaba Y, Kobayashi N, et al. Effects of rotational acetabular osteotomy on the mechanical stress within the hip joint in patients with developmental dysplasia of the hip: a subject-specific finite element analysis. Bone Joint. 2015;97-B(4):492-7.
14. Phillips AT, Pankaj P, Howie CR, et al. Finite element modelling of the pelvis: inclusion of muscular and ligamentous boundary conditions. Med Eng Phys. 2007;29(7):739-48.
15. Goel VK, Kim YE, Lim TH, et al. An analytical investigation of the mechanics of spinal instrumentation. Spine (Phila Pa 1976). 1988;13(9):1003-11.
16. Shi D, Wang F, Wang D, et al. 3-D finite element analysis of the influence of synovial condition in sacroiliac joint on the load transmission in human pelvic system. Med Eng Phys. 2014;36(6): 745-53.
17. Kim HJ, Chun HJ, Kang KT, et al. A validated finite element analysis of nerve root stress in degenerative lumbar scoliosis. Med Biol Eng Comput. 2009;47(6):599-605.
18. Hashimoto K, Aizawa T, Kanno H, et al. Adjacent segment degeneration after fusion spinal surgery-a systematic review. Int Orthop. 2019;43(4):987-93.
19. Denis F, Sun EC, Winter RB. Incidence and risk factors for proximal and distal junctional kyphosis following surgical treatment for Scheuermann kyphosis: minimum five-year follow-up. Spine (Phila Pa 1976). 2009;34(20):E729-34.
20. Untch C, Liu Q, Hart R. Segmental motion adjacent to an instrumented lumbar fusion: the effect of extension of fusion to the sacrum. Spine (Phila Pa 1976). 2004;29(21):2376-81.
21. Rahm MD, Hall BB. Adjacent-segment degeneration after lumbar fusion with instrumentation: a retrospective study. J Spinal Disord. 1996;9(5):392-400.
22. Onsel C, Collier BD, Kir KM, et al. Increased sacroiliac joint uptake after lumbar fusion and/or laminectomy. Clin Nucl Med. 1992;17(4):283-7.
23. Ivanov AA, Kiapour A, Ebraheim NA, et al. Lumbar fusion leads to increases in angular motion and stress across sacroiliac joint: a finite element study. Spine (Phila Pa 1976). 2009;34(5):E162-9.
24. Offierski CM, MacNab I. Hip-spine syndrome. Spine (Phila Pa 1976). 1983;8(3):316-21.
25. Tateuchi H, Akiyama H, Goto K, et al. Sagittal alignment and mobility of the thoracolumbar spine are associated with radiographic progression of secondary hip osteoarthritis. Osteoarthr Cartil. 2018;26(3):397-404.
26. Esposito CI, Miller TT, Kim HJ, et al. Does degenerative lumbar spine disease influence femoroacetabular flexion in patients undergoing total hip arthroplasty? Clin Orthop Relat Res. 2016;474(8): 1788-97.